Effect of Hygrothermal Aging on the Fracture of Composite Overlays on Concrete

JED LYONS,[1] DOROTHY LAUB AND VICTOR GIURGIUTIU
Department of Mechanical Engineering
University of South Carolina
Columbia, SC 29208

MICHAEL PETROU
Department of Civil and Environmental Engineering
University of South Carolina
Columbia, SC 29208

HANADI SALEM
Department of Mechanical Engineering
American University in Cairo
Cairo, Egypt

ABSTRACT: This research assessed the effects of elevated temperature and humidity exposures on the durability of fiber reinforced epoxy composite overlays on concrete substrates. Modified double cantilever beam samples were used to determine the Mode I strain energy release rate of the composite-to-concrete bond after exposure to temperatures of 23°, 60° or 100°C, humidity levels of 50 or 95% RH, and times up to 40 days. The only statistically significant degradation in toughness was observed after exposure to the 100°C, 95% RH environment. However, chemical changes in the matrix occurred during this extreme exposure condition that may not represent the in-service aging of composite-repaired concrete structures.

KEY WORDS: composites, concrete, civil infrastructure, bond, durability, toughness, strain energy release rate.

[1]Author to whom correspondence should be addressed.

INTRODUCTION

THE BROAD OBJECTIVE of this research is to assist in the development of in-situ repair techniques for aging civil infrastructure. It is well established that exposure to serviceable environments affects the mechanical properties, color, gloss, and life expectancy of many polymeric materials [1–3]. Of particular interest for materials used to rehabilitate infrastructure are the effects due to humidity and heat on their mechanical properties. Epoxies are favored over many other polymers for their adhesiveness, high molecular mobility, and corrosion resistance [4,5]. For these reasons, they are commonly used as protective coatings, adhesives, and with fiberglass to make laminates. There is very little shrinkage in curing because epoxies do not release any reaction products. With fiber reinforcements, they can be applied directly to the structures and allowed to cure without forming any internal stresses. These properties make epoxies excellent resins to be used for the rehabilitation of bridges or other structures. However, they do show some oxidation and absorption of water. It is therefore important to determine the effects of oxidation and water absorption that may occur during the expected life of the epoxy fiberglass composite.

Limited numbers of studies have been conducted on the durability of composite rehabilitation of construction materials. Karbhari and Shulley [6] investigated the durability of the bond between composites and steel. They studied three types of glass and two carbon FRPC systems. The 25.4 by 203 mm specimens were subjected to six different environments: ambient, synthetic sea water at 25°C, hot water at 65°C, water at 25°C, freezing at –18°C, and freeze thaw. Bond durability was assessed using the wedge-test, ASTM D3762. The overall results showed that the rehabilitation/repair systems performed well, and they have great potential. The hot-water environment (65°C) was the most aggressive environment, reducing significantly the bond durability of all tested systems. In a similar study, Karbhari and Engineer [3] studied the durability of composite rehabilitation schemes for concrete using a peel test. Concrete blocks of size 22.86 cm length, 15.24 cm width and 2.54 cm depth were rehabilitated using two glass and two carbon FRPC schemes. The specimens were subjected to five different environments for sixty days, namely: ambient conditions, fresh water at 20°C, synthetic sea water at 20°C, freezing at –15.5°C, and freeze thaw. It appears that there was very little effect of short-term exposure to water or sea water on the Mode I component of interfacial fracture energy while Mode II component was significantly reduced. Freezing or freeze thaw exposures caused an increase to both components of the interfacial fracture energy mainly due to additional stiffening on the peel test itself.

The effect of water absorption on composite laminates has also been investigated [7]. Epoxy/graphite and epoxy/Kevlar composite panels were placed in a humid environment and when a weight gain of 1% was observed, the panels were removed and fatigued. Moisture conditioning was observed to increase the resid-

ual strength of plain laminates, but reduced the strength of laminates with epoxy/S-glass buffer strips. Experiments have also been conducted to determine the effects of thermo-oxidative aging on composite laminates [8]. In that research, two different epoxies were used as the matrix material with carbon fibers, making two different composites. Tensile, compressive, and fracture tests were conducted to evaluate the mechanical properties. It was observed that fiber bridging across the crack increased with aging time. This fiber bridging increased the critical Mode I strain energy release rate, G_{IC}, of the composites. It was concluded that degradation of the epoxy matrix resulted in this increase of fiber bridging because at crack initiation, G_{IC} is matrix dominated.

To develop a test suitable for evaluating the effects of moisture and thermo-oxidation on the fracture of composite overlays on concrete, it is necessary to evaluate the type of in-service loading that structures are most likely to be subjected. A crack can experience three types of loading. These types are Mode I, a tensile (or opening) loading applied to the crack tip, Mode II, in plane shear loading, and Mode III, out-of-plane shear (or tearing) loading. The two most important loading modes that must be considered are Modes I and II, since natural disasters such as earthquakes impart both modes at the interface between the overlay and the concrete substrate. Processes such as cyclic freeze-thaw and vandalism impart a Mode I loading. A freeze-thaw cycle, especially in humid conditions, allows moisture to enter the cracks and, upon freezing, the water expands. This expansion places an opening force on the crack. Likewise, vandalism would also impart a Mode I loading on the crack if an attempt is made to pull the overlay of the concrete substrate. Therefore, it is useful to understand how the durability of the bond is affected under Mode I loading conditions.

There are many established test methods for determining the Mode I fracture toughness and interfacial fracture energy between adhesives and steel. For example, the ASTM standard D 3433-93 defines the procedures for using the double cantilever beam test (DCB), which may be used to quantify the strain energy release rate of the adhesive that bonds together two symmetrical metallic plates [9]. While no test methods have been standardized for measuring the bond between composite and concrete, Karbhari and Engineer [3] measured the composite-concrete bond toughness with a peel test. The overlays were pulled off of the substrate at a constant rate and known angle. Rollers were used to ensure that the composite overlays peel off tangent to the roller. However, many of the composites that can be used in the rehabilitation of concrete structures are too stiff to peel off in this manner.

MODIFIED DOUBLE CANTILEVER BEAM TEST

The test method developed for this research is derived from the ASTM D3433 standard, and is thus called the Modified Double Cantilever Beam (MDCB) test.

Unlike the specimens used in the DCB test, the specimens in the MDCB test are not made of two identical beams. Instead, the composite/masonry specimens consist of a concrete substrate that is much less compliant than the fiber reinforced epoxy composite overlay to which it is bonded. The following paragraphs describe the development of the equations used to evaluate the fracture between the composite and the masonry from fracture theory [10].

An MDCB composite/masonry test specimen is illustrated in Figure 1(a). An external load, P, is applied to the composite overlay in a Mode I loading as shown. The experimental setup resembles a double cantilever beam test in that two "beams" are pulled apart from each other in an opening method. As in a DCB test, the crack length, a, is a function of the compliance and the toughness of the adhesive between the beams may be assessed. Specifically, the strain energy release rate, G, maybe written in terms of the load, P, the sample width, B, and the compliance, C, as shown in Equation (1).

$$G = \frac{P^2}{2B}\frac{\partial C}{\partial a} \tag{1}$$

Because geometry and loading conditions can be directly measured, an experimental value for the strain energy release rate may be determined from Equation (1) if compliance can be described as a function of crack length.
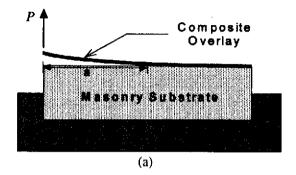
In the present case of a thin composite bonded to the surface of a massive concrete substrate, the deflection and compliance of the concrete substrate is neglected. The composite overlay is modeled as a simple beam. The beam length, at any time, is equal to the crack length, a. The deflection at the load point, δ, is given by the following equation:

$$\delta = \frac{Pa^3}{3E_{11}I} \quad \text{where} \quad I = \frac{Bh^3}{12} \tag{2}$$

and E_{11} is the elastic modulus of the composite in the longitudinal (crack growth) direction, I is the moment of inertia, B is the width, and h is the thickness of the overlay. Dividing the above equation through by P gives an expression for the compliance, Equation (3). The cubic root of compliance, therefore, varies linearly with the crack length, where the slope of the line, m, is given by Equation (4).

$$C(a) = \frac{a^3}{3E_{11}I} \tag{3}$$

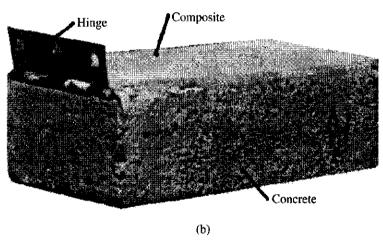$$m = \left(\frac{1}{3E_{11}I}\right)^{1/3} \tag{4}$$

(a)

(b)

Figure 1. *Modified double cantilever beam test used to peel a composite overlay off of a concrete masonry substrate. (a) Schematic of the test method. (b) Test specimen showing embedded hinge used to apply the load.*

By substituting Equations (3) and (4) into Equation (1), the strain energy release rate is given as

$$G = \frac{3m^3 a^2 P^2}{2B} \quad (5)$$

Equation (5) assumes that the composite overlay is fixed at the crack tip and that the curvature begins at that point. However, in practice, the overlay may actually have a rotational center ahead of the crack tip. The correction for this suggested in ASTM standard D 5528-94a [11], is to assume that the rotation occurs at a point ahead of the crack tip, $a + \Delta$. A least squares fit to the cubic root of compliance gives an experimental value for Δ. With the correction for crack length, the cubic root of compliance is expressed as

$$C^{1/3} = ma + \Delta \quad (6)$$

Substituting Equations (6) and (4) into Equation (1) yields

$$G = \frac{3m^3 (a + \Delta/m)^2 P^2}{2B} \quad (7)$$

Accordingly, the focus of this research is to develop a test method that evaluates Mode I fracture resistance of the FRPC overlays on masonry substrate systems.

EXPERIMENTAL PROCEDURES

Materials

A commercial source that develops and manufactures tailored composite products for a variety of applications donated the matrix and reinforcement materials used in this research. The matrix material was a two part polyamide-cured trowelable epoxy. The reinforcement consisted of a non-woven scrim grid with 1 cm spacing between reinforcement bundles. In the process used to produce the reinforcement, glass fiber tows are wet-out with a flexibilized epoxy matrix and laid-out to cure into a two-dimensional grid pattern.

The bricks used were purchased from a local supplier and met ASTM specifications for concrete masonry units [12]. They were put in an oven at 100°C for at least 24 hours to remove any moisture. The top and bottom surfaces of the bricks were sanded using an electric sander until both surfaces were smooth. Thorough cleaning of the brick surfaces was conducted using a wire brush and a vacuum cleaner.

Specimen Preparation

In the first step of sample preparation, a 38 mm wide strip of masking tape was applied at one end of the brick to serve as a pre-crack. Then, the primed surface of a 50 mm long steel hinge was placed face up on the taped end of the brick. A wooden spatula was used to spread an even layer of epoxy over the dust free brick and hinge surfaces. One layer of reinforcement was placed squarely over the epoxy and was pressed in firmly with the fingertips until the epoxy was observed to flow up through all the holes in the grid. Two more layers of epoxy and reinforcement were adhered to the sample and a final layer of epoxy was smoothed over the top of the fiberglass composite. These reinforcement grids are very open so that the epoxy easily penetrates through them. Approximately 100 grams of epoxy were used for each sample, yielding a final volume fraction of the reinforcement grid of approximately 7%. The samples were allowed to cure for at least one week before excess epoxy was mechanically removed from their edges. Figure 1(b) shows a completed MDCB specimen.

Environmental Exposure

Samples were randomly selected from each batch and placed into one of five environmental conditions (EC) as listed in Table 1. The samples were aged in the laboratory and at elevated temperatures in a forced air convection oven (laboratory humidity) or an environmental chamber (elevated humidity). It was desired to pull samples out to be tested after 2, 5, 10, 20, and 40 days of exposure.

Mechanical Testing

A test fixture was fabricated to allow for mixed mode testing, although only Mode I results are presented here. The bottom part of the test fixture, consisting of a trough and side clamps for securing the brick, was attached to the piston of a servo-hydraulic universal testing machine. The top part of the loading fixture, consisting of a clamp for the hinge, was attached to the machine's load cell through a

Table 1. The environmental conditions.

Environmental Condition	Temperature (°C)	Humidity (%)
EC 1	LAB	LAB
EC 2	60	LAB
EC 3	60	95
EC 4	100	LAB
EC 5	100	95

pin and clevis. A loading rate of 0.025 mm/sec was used to lift the precracked end of the composite off of the substrate. Load and load-point displacement measurements made every 12 mm of crack growth were used for calculating the strain energy release rate.

RESULTS

Test Method Validation

The validity of the test depends on the correctness of the assumptions made in the development of the characterizing equations. There were three major assumptions: a) the crack front was straight so that the crack length could be determined from surface measurements, b) dissipative processes were negligible, i.e., the energy went into the formation of new surfaces, and c) the composite overlay behaved like a simple linearly elastic beam.

The crack length on each side of the sample was measured to an accuracy of 1 mm and the average of these two measurements was used to calculate G. The actual shape of the crack front is therefore very important in determining the validity of the test results. If crack tunneling takes place, for example, the crack length estimated from surface measurements will be much smaller than the actual crack length. For that reason, some tests were interrupted and black paint was injected into the crack front using a hypodermic needle while the crack was open. Surface measurements of the crack tip location at that time were also taken. The overlay was removed after the paint had dried. The results from these paint injection tests provide good reason to believe that the measurements were accurate. In all cases, the crack shape was linear and no crack tunneling was observed. Therefore, using the average of the crack lengths as measured on both sides of the specimen is an accurate estimate of the crack length.

For most of the tests, the crack opening displacement was increased monotonically. However, in order to quantify the role of dissipative deformation mechanisms during crack extension, several samples were subjected to periodic unloading. In these cases, instead of holding the position constant while marking the crack lengths, the loading direction was reversed. The crack length was measured on both sides of the sample immediately after unloading began. Unloading continued at the same rate as the loading until the force was approximately half of that before the unloading began. As shown by the typical results presented in Figure 2, very little hysteresis was observed during unloading. The unloading curves also tended towards the origin, indicating that the composite behaved elastically. Hysteresis did appear to increase with crack length, suggesting that the calculations of G after large crack growth may be less accurate.

Describing the composite overlay as a simple linear elastic beam is accurate if the beam thickness is constant and if the cubic root of compliance varies linearly
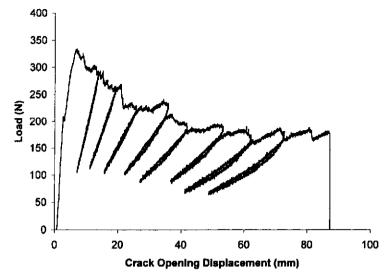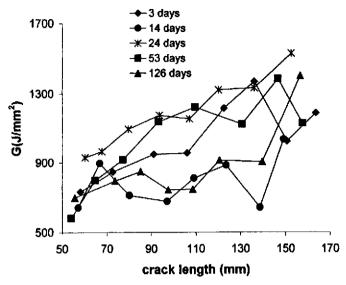
Figure 2. *Typical load-displacement curve including unloading.*

with the length of the beam. As fabricated, there was negligible variation in the thickness of the composite overlay. However, the thickness did not remain constant during testing because sometimes the crack path was through the composite. A non-negligible difference in thickness or width, however, would have resulted in a poor relation between compliance and crack length. Assumed in Equation (5) is that the cubic root of compliance varies linearly with crack length. The correlation coefficients, R^2 of the equation that relates $C^{1/3}$ to a [Equation (6)] ranged from 0.76 to 0.98, and averaged 0.91.

Crack Growth Resistance Behavior of Laboratory Conditioned Samples

A plot of the strain energy release rate as a function of crack extension is a crack growth resistance curve. These curves were determined from the load, deflection and crack length measurements of each sample using Equation (7). Typical crack growth resistance curves for the samples that were maintained in a laboratory environment after fabrication are shown in Figure 3. Of note, the cracks grew longer than 90 mm, the calculated G values began to increase rapidly with crack length.

Frequently, a rising G-a behavior is interpreted as an increase in the crack growth resistance of the material with increased crack length. In many of the samples tested here, the crack grew through the composite overlay layer for some portion of the test. When it did so it often grew through the fiber tows that made up the reinforcement grid, providing evidence of fiber pullout on the fracture surfaces. If these fibers remained intact and bridged the crack faces as the crack grew past

Figure 3. *Representative crack growth resistance curves for samples conditioned in the laboratory environment.*

them, then they would contribute to a crack closing force. The applied force would have to increase to overcome this crack closure force while furthering crack growth, leading to a rising *G-a* curve.

Rising *G-a* behavior also occurred with samples that did not show any evidence of fiber pullout on their fracture surfaces, however. Therefore, the reason for the increase in *G* with crack length is likely due, in part, to an increase in the amount of Mode II (shear) crack tip loading. As the load-point deflection of the composite overlay increased, a relatively large amount of bending occurred in the composite. The overlay beam deformation, therefore, could no longer be described by small deflection beam theory. As the overlay acquired curvature, an increasing amount of the load was carried in direct tension by the composite. This would cause a shift from pure tensile Mode I loading to a mixture of Mode I/II loadings, and an increase in the applied load necessary to propagate the crack.

Initiation Value of Critical Strain Energy Release Rate

The strain energy release rate was determined at a crack length of 60 mm for each sample to facilitate the analysis of results. This is designated as G_{60}. The selection of a crack length of 60 mm for comparison was somewhat arbitrary. However, at this position the embedded hinge and any other irregularities, such as voids near the hinge or reinforcement curvature at the precrack site should not affect the stresses at the crack tip. More importantly, in this region the *G-a* behav-

ior of the samples was essentially flat so that Mode I loading conditions dominated. Comparison of the mixed-mode loading condition results is precluded by the fact that the overlay opening angle was not directly measured during the experiments discussed here. However, G_{60} is a valid parameter for characterizing the fracture resistance of the material because it represents the strain energy release rate corresponding to the initiation of crack growth.

The G_{60} values for samples that were maintained in the laboratory at approximately 23°C are listed in Table 2. These results and the general behavior exhibited by the *G-a* curves in Figure 3 indicate that there was no systematic increase or decrease in the toughness values measured with respect to time after fabrication. This suggests that the composite was fully cured after processing and that subsequent aging in an ambient environment did not significantly affect its properties. There was, however, sample-to-sample variation in the results due to the hand lay-up processing method as used in this research. When the results from all of the laboratory conditioned samples are considered together, the average and standard deviation for the G_{60} toughness of the composite-concrete material system are 792 ± 225 J/mm^2. This range is consistent with the work of others [3] who have measured strain energy release rates that vary from 300 to 1000 J/m^2 for different composite overlay and concrete material systems.

Effect of Accelerated Environmental Aging

As described, samples were exposed for different times at elevated temperatures

Table 2. Strain energy release rates at 60 mm crack length for different exposure conditions.

23°C Dry		60°C Dry		60°C Wet		100°C Dry		100°C Wet	
Time (Days)	G_{60} (J/m^2)	Time (Days)	G_{60} (J/m^2)	Time (Days)	G_{60} (J/m^2)	Time (Days)	G_{60} (J/m^2)	Time (Days)	G_{60} (J/m^2)
3	749	2	857	2	344	8	552	3	323
5	910	2	685	2	377	14	845	6	289
14	714	5	614	5	801	26	925	14	630
14	943	5	790	5	610	36	716	23	318
24	930	10	754	10	645	36	895	30	683
51	940	20	1119	20	1034	40	642	40	400
53	721	21	621	21	1035	40	717	40	557
55	1274	40	925	40	642	40	504		
55	467	41	764	40	520				
112	673								
126	725								
126	897								
163	400								

(60°C or 100°C) and different humidity levels (laboratory ~ 50% RH or controlled 95% RH). Typical crack growth resistance curves for these four conditions are presented in Figures 4–7, while tabulated G_{60} values are presented in Table 2. Again, rising G values with crack extension were observed. Also, there is no apparent systematic effect of time of exposure on the shapes of the G-a curves or the values of G_{60}. This suggests that if changes occurred in the material as a result of environmental exposure, they did so in times shorter than those investigated here. Therefore, excluding time as a variable and calculating the average G_{60} for each condition allows a comparison of the effects of the different environmental variables.

The average G_{60} for each environmental exposure condition is plotted in Figure 8. The error bars in this figure represent one standard deviation in the results. It appears that the mean value of the strain energy release rate was not affected by exposure to elevated temperatures, provided that humidity was not added to the exposure environment. The average G_{60} value for the samples aged in a 60°C, wet environment is slightly lower than that of the laboratory conditioned samples, but due to the variability in the test results this difference could not be statistically proven. However, the average G_{60} for the samples exposed at 100°C and 95% RH is significantly lower than that of the laboratory conditioned samples. This was verified with a t-test at a 95% confidence interval. Similar results were obtained by Karbhari and Shulley [6]. There, 65° water significantly reduced the bond durabil-
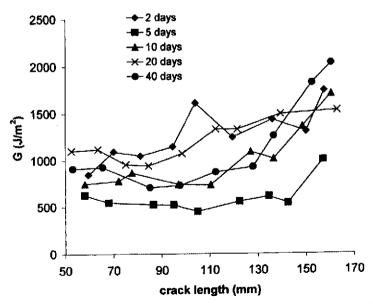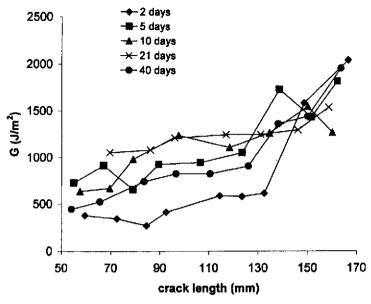

Figure 5. *Representative crack growth resistance curves for samples conditioned in the 60°C, wet environment.*

Figure 4. *Representative crack growth resistance curves for samples conditioned in the 60°C, dry environment.*
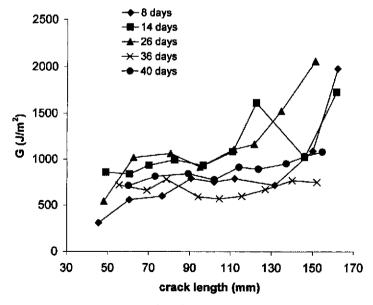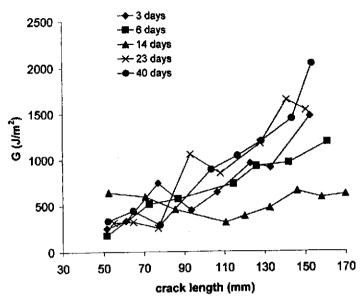

Figure 6. *Representative crack growth resistance curves for samples conditioned in the 100°C, dry environment.*

Figure 7. Representative crack growth resistance curves for samples conditioned in the 100°C, wet environment.
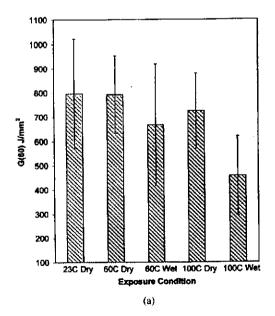

(a)

Figure 8. Comparison of the results after environmental exposure: (a) average initiaion values of strain energy release rates, (b) predominant fracture paths.

(b)

Figure 8 (continued). Comparison of the results after environmental exposure: (a) average initiaion values of strain energy release rates, (b) predominant fracture paths.
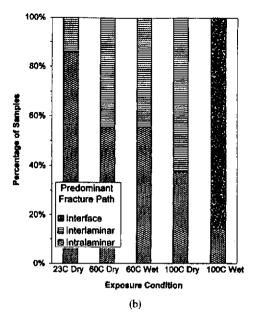
ity of all tested systems.

Differences in the crack growth resistance after environmental exposure are related to differences in the crack propagation path in the samples. In this research, the cracks were observed to propagate in four different ways. The least common involved fracture through the concrete substrate, where small pieces of the concrete substrate adhered to the composite after it was peeled off. This was observed on only about 15% of the samples tested, but it did occur in some samples in each environmental condition investigated. When it did occur, it accounted for 10% or less of the fracture surface. No correlation could be found between samples that partially failed in this manner and the measured strain energy release rates.

The most common fracture path was interlaminar, which involved separation of the composite matrix at the plane of the fiber grid reinforcement. Also observed in a number of samples was an intralaminar failure mechanism. In these cases, the cracks grew through the fiber bundles in the reinforcement grid, splitting the composite layer in two. These two fracture paths were predominant in the samples conditioned in the laboratory and in those exposed to 60°C dry, 60°C wet, and 100°C dry environments, as shown in Figure 8. The fact that interface failure between the composite overlay and the concrete substrate did not occur in these samples indicates that the interface bond strength was more than adequate.

Most of the samples exposed to the 100°C wet environment fractured differ-

ently than the others. What was observed was a fairly clean separation of the composite from the concrete. This interface failure indicates that the bond between the composite resin and the concrete was degraded by this environmental exposure. The cause of this degradation is likely related to chemical changes in the resin, because a color change was observed in the composite after even short exposure times (the specimens obtained a brownish tinge). Based on these observations, the degradation that occurred in this extreme environmental exposure condition may not be representative of the various degradation mechanisms that occur during actual aging conditions of composite-repaired concrete structures in the field.

CONCLUSIONS

A test method, based on cantilever beam theory, has been proposed that can be used to evaluate the crack growth resistance behavior of composite overlays on concrete substrates. Validation of the method is supported by the results, i.e., the cubic root of the overlay compliance varied linearly with crack length, the unloading curves tended back towards the origin during crack growth, the hysteresis was negligible during unloading, and the crack front shape remained straight. The initiation value of the critical strain energy release rate, G_{60}, was useful for investigating the effect of environmental exposure on the composite/concrete material system. No correlation was observed between G_{60} and the time of exposure. In addition, no statistically significant degradation in mechanical properties was observed after exposure to 60°C wet, 60°C dry or 100°C dry environments. A significant drop in the toughness between the composite overlay and the concrete substrate was observed after exposure to the 100°C wet environment. However, chemical changes in the matrix occurred during this extreme environmental exposure condition that may not be representative of the actual aging of composite-repaired concrete structures in the field.

ACKNOWLEDGMENT

REFERENCES

1. Buck, S., Lischer, D., and Nemat Nasser, S. 1998. "The Durability of E-Glass/Vinyl Ester Composite Materials Subjected to Environmental Conditioning and Sustained Loading," *Journal of Composite Materials*, 32:874–892.
2. Prian, L., Pollard, R., Sham, R., Mastropietro, C., Gentry, T., Bank, L., and Barkatt, A. 1997. "Use of Thermogravimetric Analysis to Develop Accelerated Test Methods to Investigate Long-Term

Environmental Effects on Fiber-Reinforced Plastics," *Polymeric Composites*, 2:206–222.
3. Karbhari, V. M. and Engineer, M., 1996. "Investigation of Bond between Concrete and Composites: Use of a Peel Test," *Journal of Reinforced Plastics and Composites*, 15:208–227.
4. Progelhof, R. and Throne, J. 1993. *Polymer Engineering Principles: Properties, Processes, Tests for Design*, Hanser Publishers, 391.
5. Anon. 1999. "Repairing Columns without Using Forms," *Concrete International*, Vol. 21, 3:82.
6. Karbhari, V. and Shulley, S., 1995. "Use of Composites for Rehabilitation of Steel Structures—Determination of Bond Durability," *Journal of Materials in Civil Engineering*, 7:239–245.
7. Bigelow, C., 1989. "Effects of Fatigue and Environment on Residual Strengths of Center-Cracked Graphite/Epoxy Buffer Strip Panels," *Experimental Mechanics*, 29:90–94.
8. Tsotsis, T. and Lee, S., 1998. "Long-Term Thermo-Oxidative Aging in Composite Materials: Failure Mechanisms," *Composite Science and Technology*, 58:355–386.
9. American Society for Testing and Materials. 1994. *Standard Test Method for Fracture Strength in Cleavage of Adhesives in Bonded Metal Joints*, ASTM Standard D3433-94.
10. Giurgiutiu, V., Lyons, J., Petrou, M., Laub, D., and Whitley, S. 1999. "Experimental Fracture Mechanics for the Bond between Composite Overlays and Concrete Substrate," *Proceedings of International Composites EXPO'99*, May 10–13, 4D1–4D6.
11. American Society for Testing and Materials. 1994. *Standard Test Method for Mode I Interlaminar Fracture Toughness of Unidirectional Fiber-Reinforced Polymer Matrix Composites*, ASTM Standard D 5528-94a.
12. American Society for Testing and Materials. 1996. *Standard Specification for Loadbearing Concrete Masonry Units*, ASTM Standard C 90–96a.